Elimination of D-band in Raman spectra of double-wall carbon nanotubes by oxidation

S. Osswald [a], E. Flahaut [b], H. Ye [a], Y. Gogotsi [a,*]

[a] Materials Science and Engineering Department and A.J. Drexel Nanotechnology Institute, Drexel University,
3141 Chestnut Street (383 CAT), Philadelphia, PA 19104, USA
[b] Centre Interuniversitaire de Recherche et d'Ingénierie des Matériaux, UMR CNRS 5085, Université Paul Sabatier, 118 Route de Narbonne,
31062 Toulouse, France

Abstract

In this Letter, we present an in situ Raman spectroscopy study of oxidation-induced changes in the structure and composition of double-wall carbon nanotubes (DWCNTs). Above 480 °C, the intensity of the D band decreases to less than 0.01% of the G band intensity, when measured using the 780 nm laser excitation. The D band was absent from the Raman spectra recorded with the 514.5 nm excitation. Thermogravimetric analysis and high-resolution transmission electron microscopy are used to explain the observed results. We conclude that oxidation provides a purification method for the DWCNT which leads to a sample containing tubes having nearly clean surfaces without disordered carbon.
© 2004 Elsevier B.V. All rights reserved.

1. Introduction

Double-wall carbon nanotube (DWCNT) is the most basic member of the multi-walled carbon nanotube (MWCNT) family [1] which can be produced in significant quantities [2]. These tubes consist of two concentric cylindrical graphene layers and their range of diameters is comparable to that of single-walled carbon nanotubes (SWCNT). Several methods for producing DWCNT have been reported, such as catalytic chemical vapour deposition (CCVD) [1–3], arc discharge [4] or heating C_{60} molecules encapsulated in SWCNT [5].

Unfortunately, commercially viable methods such as CVD or arc discharge lead to products which contain catalyst particles and 'amorphous' carbon. The products also contain some SWCNT and MWCNT along with DWCNT. Of course, the diameter distribution and also the content of different tubes in the raw product vary between the different synthesis methods. There exists no single purification process which would remove all impurities and separate DWCNT from other types of tubes. While catalyst particles can be eliminated by acid treatments [1,6,7], the amorphous carbon and the unwanted SWCNT can also be removed by oxidation in flowing or static air [1,6–9]. Thermogravimetric analysis (TGA), which shows changes of mass during oxidation processes, has been used to determine the oxidation purification conditions [10].

However, TGA alone does not provide information on what is removed from the sample by oxidation. Raman spectroscopy provides a powerful method for characterization of the carbon structure [11]. Similar to the Raman spectra of SWCNT, DWCNT exhibit three characteristic bands: the tangential (vibrations along the tube axis) stretching G mode (1500–1600 cm^{-1}), the D mode (~1350 cm^{-1}) and the radial breathing mode RBM (100–400 cm^{-1}) [11–14]. While the frequency of the RBM is inversely proportional to the tube diameter, the tangential stretching mode weakly

depends on the diameter of the nanotube [15]. D band in amorphous or disordered carbon is assigned to a double-resonance Raman effect in sp^2 carbon [16]. The contribution of defects in the tube walls and other forms of carbon, such as rings, to the D band is still not completely understood. Raman spectroscopy can provide real-time monitoring of changes in the sample's structure and composition.

In this Letter, we present the results of an in situ Raman spectroscopy study of oxidation of DWCNT which were produced by a CCVD method. The goal of the work was to select the oxidation conditions leading to the removal of amorphous carbon by monitoring the intensity of the D band in Raman spectra.

2. Experimental

The DWCNT were produced by the CCVD method using a $Mg_{1-x}Co_xO$ solid solution catalyst containing molybdenum oxide with the elemental composition $Mg_{0.99}Co_{0.0075}Mo_{0.0025}$ [2]. The as-produced CNTs contained a very low amount of amorphous carbon, present only as deposits on some of the tubes' outer wall.

HRTEM observation of the sample showed 77% DWCNTs, 18% SWCNTs and 5% TWCNTs. The diameter distribution of the DWCNT ranged from 0.53 to 2.53 nm for inner tubes and from 1.2 to 3.23 nm for outer tubes, while the diameters of the SWCNT reached 1.1–2.7 nm [2]. The sample was heated in a Linkam THMS 600 heating stage in static air from 20 to 600 °C at 5 °C/min. The sample was held for 4 min at every measurement point. The stage was calibrated by using the melting points of $AgNO_3$ (209 °C), Sn (232 °C), KNO_3 (334 °C), and $Ca(OH)_2$ (580 °C). In every case, the difference between the measured and expected melting point did not exceed 2 °C.

The spectra were acquired with a Raman micro spectrometer (Renishaw 1000) using an Ar ion laser (514.5 nm) and a diode laser (780 nm) in back-scattering geometry. We used a 20× objective with a spot size of ~5 μm in diameter, which included a large number of tubes, providing statistically reliable results. A low laser power density was used on the sample (laser power <2 mW) to avoid laser heating of the tubes. This low power density was achieved by filtering and/or defocusing the laser beam at the sample surface. Spectra were acquired with 50 °C steps in the range from 50 to 350 °C, followed by 25 °C steps from 350 to 400 °C and concluded with 10 °C steps from 400 to 600 °C. After reaching the desired maximum temperature, the sample was cooled down at 20 °C/min until reaching 80 °C and then cooled at 10 °C/min to room temperature. The heating/cooling cycle was repeated 15 times on different samples from two different DWCNT batches to obtain statistically reliable data. The same

heating procedure was used for every repetition and each time the experiments were stopped after reaching the maximum temperature.

The TGA was performed with a SETARAM TAG24 thermobalance. In the TGA experiments, the sample was heated in static air from 25 to 600 °C at 5 °C/min continuously up to 400 °C. To simulate the heating conditions of the in situ Raman study, 4-min isothermal steps were performed at 400, 420, 430 and 440 °C and 8-min steps were used at 460 and 500 °C. The total heating time in the stepwise experiments with 5 °C/min heating rate was comparable to the continuous heating rate of 3 °C/min.

3. Results and discussion

Fig. 1 shows the D and G band range of the Raman spectra of DWCNT sample recorded during heating. Prior to heating, the G band can be well fitted with Lorentzian peaks at 1593 and 1568 cm^{-1}, and a broad Gaussian peak at 1525 cm^{-1} (Fig. 2a) for 514.5 nm; Lorentzian peaks at 1592 and 1564 cm^{-1}, and broader Gaussian peaks at 1548 and 1519 cm^{-1} for the 780 nm laser wavelength. Note that only in the case of Fig. 2, a baseline correction was used in the frequency range 100–700 cm^{-1} to correct the influence of the filter for
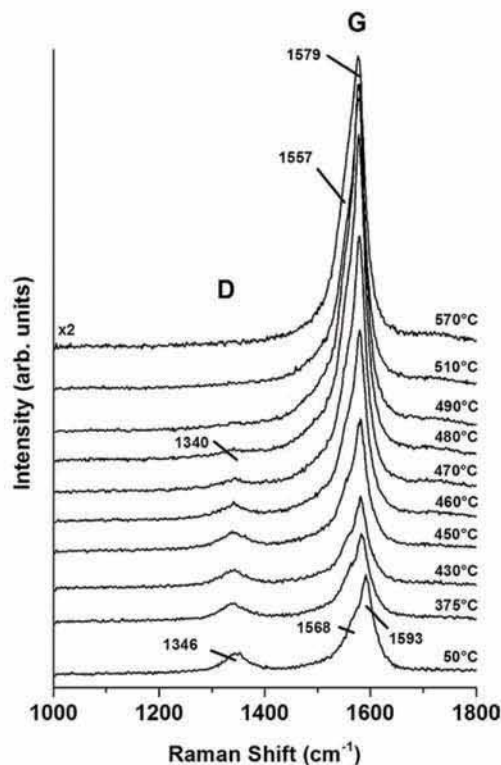

Fig. 1. In situ Raman spectroscopy study of the changes in the D and G band of DWCNT during oxidation (514.5 nm laser excitation wavelength).
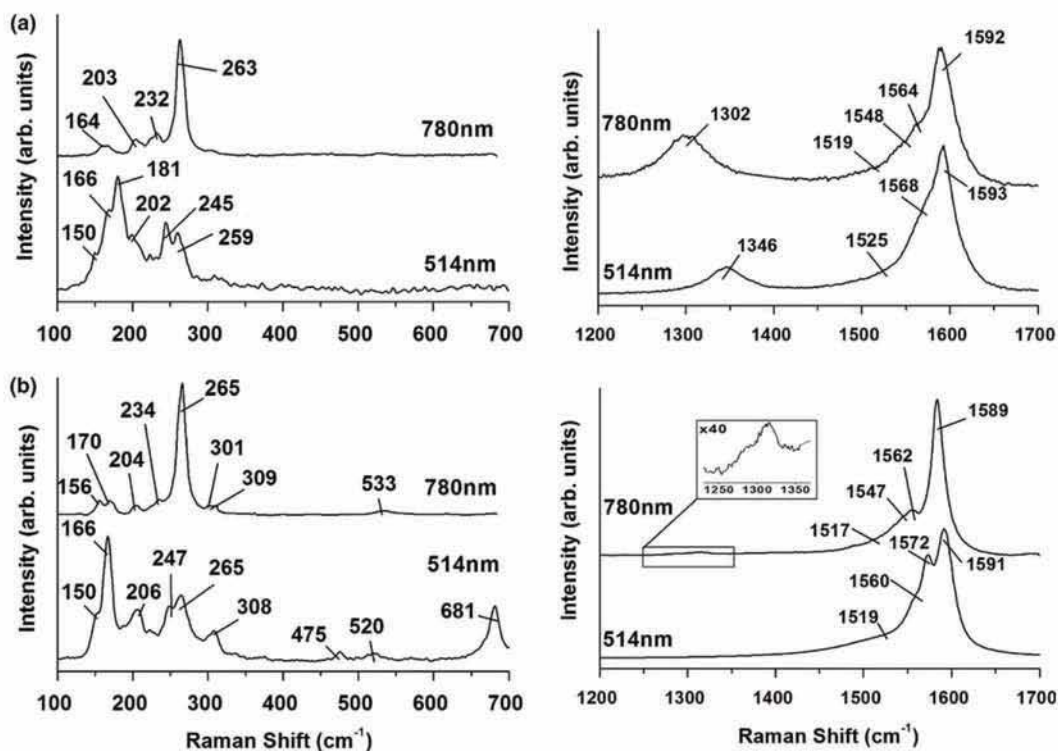
Fig. 2. Raman spectra of DWCNT using 780 and 514.5 nm laser excitation obtained (a) before and (b) after oxidation. Intensities of the spectra have been adjusted to improve presentation.

the Rayleigh peak to the spectra in the frequency range from 0 to 200 cm^{-1}. While the narrower Lorentzian peaks are ascribed to the semiconducting nanotubes, the broader peaks are attributed to the metallic tubes [17,18] or overlapping of several peaks arising from tubes with similar diameters.

In Fig. 1, it can be shown that the D peak, which is usually attributed to disordered carbon, starts to decrease at ~430 °C until it completely disappears at around 510 °C. This peak is present in the sample even if the amount of disordered carbon is very low. D band in nanotubes may also originate from defects in the tube walls and was observed in some nanotube samples that did not contain amorphous carbon. For example, we observed it in purified MWCNT samples. A linear downshift of all peaks was observed with increasing temperature, but the slope varies for different peaks. The value of the thermal shift was reported to be 0.03 cm^{-1}/°C for SWCNT [13,19]. Our measurements conducted on high purity natural graphite (G band at 1580 cm^{-1}) led to the value of 0.024 cm^{-1}/°C. The present experiment for the DWCNT, using 514.5 nm wavelength excitation, showed a downshift of 0.029 cm^{-1}/°C for the 1568 cm^{-1} peak and a value of 0.026 cm^{-1}/°C for the 1593 cm^{-1} peak (Fig. 2b), which are within the expected range.

Another important observation is that the intensity changes of the D and G bands at high temperatures follow different trends. The initial decrease of the I_D/I_G ratio is mainly due to the increase of the G band intensity. The intensity of the G band starts to increase at ~440 °C, soon after noticeable weight loss is recorded on the thermogravimetric curve (Fig. 3), and reaches a maximum around 500 °C and then it decreases again (Fig. 3). As seen in Fig 3a, the decrease in D band intensity occurs at temperatures 20–30 °C higher that the increase in G band intensity in most experiments. An explanation for the early intensity increase of G band may be the possible removal of hydrocarbons (the tube synthesis was conducted in a hydrogen-containing atmosphere) and disordered carbon, which were shielding the Raman signal from the as-received tubes. It is supported by a significant weight loss observed in this temperature range (Fig. 3b). Some variations in the temperature difference between the G and D band changes observed in our experiments may be due to a different number or packing density of nanotubes as well as different amounts of amorphous carbon present within the analyzed area. On the other hand, there might be some temperature effects on the C=C bond vibrations which may react differently during heating with respect to the curvature and the influence of temperature on the bond softening [20]. The fact that the G band's absolute intensity starts to increase at about the same temperature as the D band decreases seems to support the former hypothesis. Further evidence is provided by the fact that a higher intensity (200–300%) of G band was observed after cooling to room-temperature in every experiment. When an already oxidized sample was used
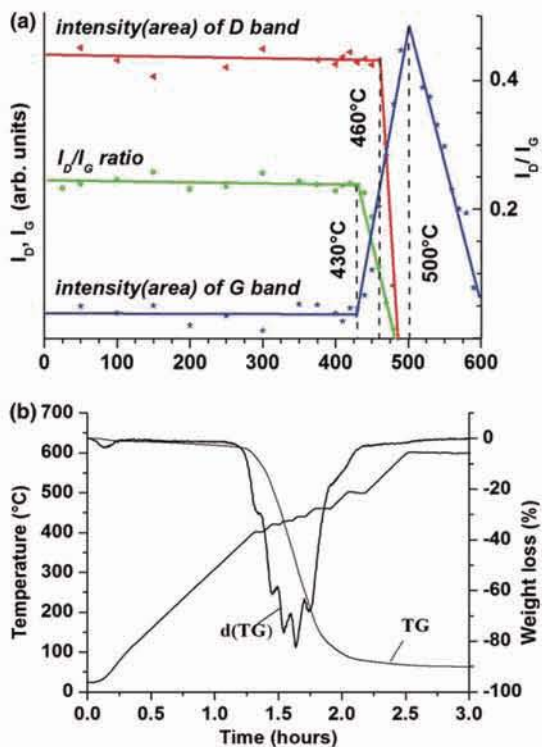
Fig. 3. (a) Comparison of intensity changes in the D and G bands during oxidation (measured with 514.5 nm laser wavelength) and (b) TGA curves obtained by heating a DWCNT sample in air.

for the in situ Raman study, no increase of G band was observed. In this case, there was no disordered carbon on the tube surface which could influence the Raman signal of the tubes.

Fig. 2 shows the Raman spectra taken at room-temperature before and after heating. This graph also demonstrates that the splitting of the G band is more pronounced after heating and that the shift of the peaks due to heating is not completely reversible. This may again be due to removal of amorphous carbon and the most defective tubes. It has been reported that the G band at 1590 cm^{-1} does not depend on the tube diameter [15]. Thus, its position should not change after oxidation of smaller tubes as a result of a decrease of their contribution to the total intensity of G band. The lower frequency component of the G band (peaks at or below ~ 1570 cm^{-1}) depends on the diameter of the tubes. The oxidation of the smaller tubes leads to a change in the lower frequency peaks while the peak at 1590 cm^{-1} shows only little shift (Fig. 2). RBM show no significant changes, thus tube size distribution have not been changed. This shows that tubes were not selectively oxidized or damaged in our process, in spite of the fact that up to a 90% weight loss was observed in some experiments (Fig. 3b).

The most noticeable effect was the near complete disappearance of the disorder induced D band after oxidation (Figs. 1–3). Using the 514.5 nm laser, the D band is

not observed at all above 510 °C. For the 780 nm laser, which produces the largest D band intensity, the I_D/I_G ratio decreases from 0.43 before heating to <0.015 after oxidation. The experiments also show that complete D-band removal is possible at lower temperatures (350–400 °C) by using a longer isothermal exposure time or a slower heating rate. These results show that in the case of DWCNT, the D band originates only from the amorphous carbon in the sample (even if present only in low amount) and not from the defects in tube walls. While the concentration of defects probably increases during the oxidation, the disordered carbon and associated D band, disappears. In similar experiments with CVD MWNT of about 10 nm in diameter, the phenomenon could not be observed after heating to 600 °C, when amorphous carbon had been removed. In the case of MWNTs, the D band probably originates primarily from defects in the tube walls. All the amorphous carbon is oxidized at temperatures below 600 °C as well as some nanotubes. However, the oxidation under our conditions has never eliminated all nanotubes. The composition of the sample at the end of the measurement depends on the analyzed spot, but comparison of RBM modes before and after oxidation (Fig. 2) shows that only insignificant changes in the distribution of tube diameters could be observed. Thus, removal of amorphous carbon is possible with minimal loss of tubes and change in diameter distributions in the sample. This cannot be explained by insufficient air supply; control experiments with open or closed valves show that there was no air shortage in the in situ Raman experiments. Also, all catalytic material was oxidized forming primarily cobalt oxide, which produced bands at 475–680 cm^{-1} in the Raman spectra of nanotubes after oxidation (Fig. 2b). The positions of Raman bands of Co_3O_4 reported in literature are 182, 460, 505, 600 and 670 cm^{-1} [21] and their relative intensities are in agreement with our observations (the strongest band is at ~ 680 cm^{-1}).

Fig. 4 shows TEM images of the DWCNT samples before (a,b), after oxidation (c,d) and after additional acid treatment (e,f) to remove catalyst particles from the sample. Two images are shown for each sample at low and high magnification, respectively. Fig. 4b shows that some amorphous carbon is present in the form of a deposit in some places in the sample before oxidation; it must be noted that Fig. 4b is not representative of the whole sample, which is mainly clean of amorphous carbon deposit. After oxidation (Figs. 4c and d), the disordered carbon is completely removed and only catalyst particles are left next to the nanotubes. The catalysts were oxidized to form Co_3O_4, as shown in Raman spectra (Fig. 2b), for which Raman peaks are strongly excited by the 514 nm laser. These oxide particles are larger than the initial nanometric metal catalytic particles due to coalescence and likely volume increase upon oxidation. Also, the content of particles in the sample
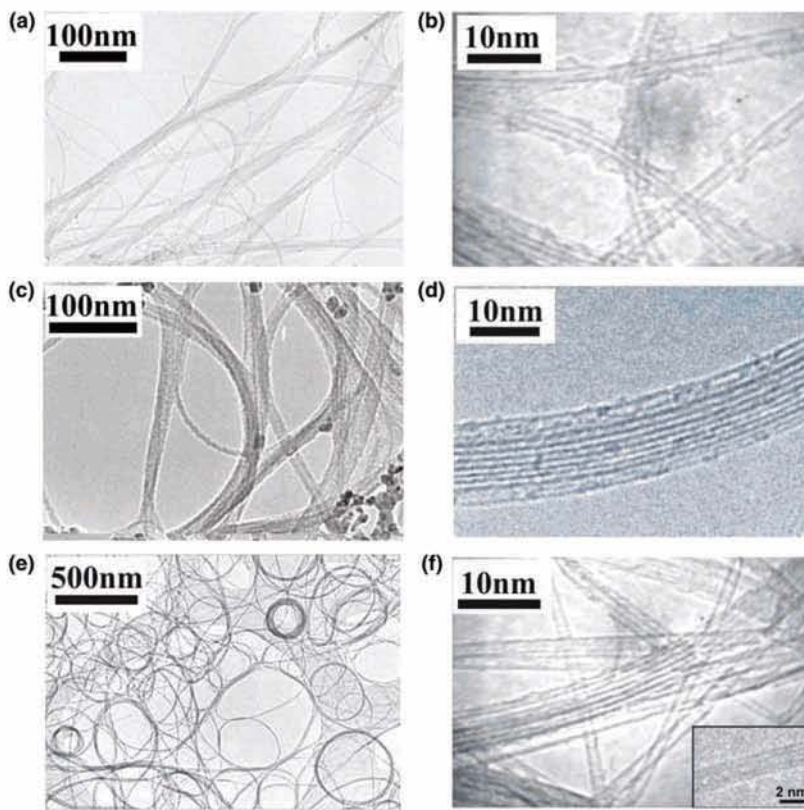
Fig. 4. Low-resolution (left panel) and high-resolution (right panel) TEM images of the DWCNT sample (a,b) before, (c,d) after oxidation and (e,f) after oxidation followed by acid treatment to remove the catalyst.

(relative to the nanotubes) seems to increase after heating to 600 °C. This may be explained by oxidation of some nanotubes in the sample as evidenced by significant weight loss observed in Fig. 3b.

While high-resolution TEM does not provide statistically reliable data on the content of defects in the tube walls, it clearly shows that the oxidized tubes are not defect-free (Fig. 4d) and do not look more perfect compared to the nonoxidized DWCNT (Fig. 4b). These wall defects, which are expected to include oxygen-terminated carbons, should provide highly reactive sites on these tubes. This may be useful for composites and biomedical applications, when surface interactions with the environment are important. However, these defects did not cause a double-resonance effect and did not produce a D band in Raman spectra (Fig. 2b). Acid treatment for removing the catalyst particles after the oxidation (Figs. 4e and f) leads to a very pure and clean sample. TEM studies of purified samples showed neither catalyst particles nor amorphous carbon, only DWCNT ready for use. If any catalyst remained, its content was well below the sensitivity limit of XRD and EDS techniques (less than one weight percent). The tubes formed rings and their mean diameter was in agreement with the experimental results and the model published by Martel et al. [22,23]. Rings have only been observed in oxidized

samples. The sonication provides the activation energy for ring formation. We had oxidized our DWCNTs at high temperature in air and then sonicated them for a short time, compared to many hours in Martel's work, to prepare TEM samples.

While the weight loss after heating to 600 °C was significant, further heating experiments in air have shown that complete removal of disordered carbon leading to the disappearance of the D band can be achieved by long-term isothermal treatment at temperatures below 400 °C and is accompanied by a much smaller weight loss (to be published elsewhere).

4. Conclusions

In situ Raman spectroscopy analysis of the oxidation of DWCNT showed a complete disappearance of the D band in the Raman spectra recorded with 514 nm laser excitation. This suggests that the D band of DWCNT is not an intrinsic feature of these tubes; the D band originates from amorphous carbon present in the sample and not from defects in the tube walls. The described oxidation process provides a method for producing nanotube samples with a very low D/G ratio (<0.015 for 780 nm excitation). The decrease or disappearance

of the D band has not been observed in MWCNT, where defects in tube walls generate a much stronger D band signal compared to DWCNT.

Acknowledgements

References

[1] E. Flahaut, A. Peigney, C. Laurent, A. Rousset, J. Mater. Chem. 10 (2000) 249.

[2] E. Flahaut, R. Bacsa, A. Peigney, C. Laurent, Chem. Commun. 12 (2003) 1442.

[3] L.J. Ci, Z.L. Rao, Z.P. Zhou, D.S. Tang, Y.Q. Yan, Y.X. Liang, D.F. Liu, H.J. Yuan, W.Y. Zhou, G. Wang, W. Liu, S.S. Xie, Chem. Phys. Lett. 359 (2002) 63.

[4] J.L. Hutchison, N.A. Kiselev, E.P. Krinichnaya, A.V. Krestinin, R.O. Loutfy, A.P. Morawsky, V.E. Muradyan, E.D. Obraztsova, J. Sloan, S.V. Terekhov, D.N. Zakharov, Carbon 39 (2001) 761.

[5] S. Bandow, T. Hiraoka, T. Yumura, K. Hirahara, H. Shinohara, S. Iijima, Chem. Phys. Lett. 384 (2004) 320.

[6] S. Gajewski, H.E. Maneck, U. Knoll, D. Neubert, I. Dorfel, R. Mach, B. Strauss, J.F. Friedrich, Diam. Relat. Mater. 12 (2003) 816.

[7] W.Z. Li, J.G. Wen, M. Sennett, Z.F. Ren, Chem. Phys. Lett. 368 (2003) 299.

[8] S. Bandow, M. Takizawa, K. Hirahara, M. Yudasaka, S. Iijima, Chem. Phys. Lett. 337 (2001) 48.

[9] E. Borowiak-Palen, T. Pichler, X. Liu, M. Knupfer, A. Graff, O. Jost, W. Pompe, R.J. Kalenczuk, J. Fink, Chem. Phys. Lett. 363 (2002) 567.

[10] J.D. Saxby, S.P. Chatfield, A.J. Palmisano, A.M. Vassallo, M.A. Wilson, L.S.K. Pang, J. Phys. Chem. 96 (1992) 17.

[11] E. Delamarche, A. Bernard, H. Schmid, B. Michel, H. Biebuyck, Science 276 (1997) 779.

[12] R.R. Bacsa, E. Flahaut, C. Laurent, A. Peigney, S. Aloni, P. Puech, W.S. Bacsa, New J. Phys. 5 (2003) 131.

[13] A.M. Rao, E. Richter, S. Bandow, B. Chase, P.C. Eklund, K.A. Williams, S. Fang, K.R. Subbaswamy, M. Menon, A. Thess, R.E. Smalley, G. Dresselhaus, M.S. Dresselhaus, Science 275 (1997) 187.

[14] H. Kuzmany, W. Plank, M. Hulman, C. Kramberger, A. Gruneis, T. Pichler, H. Peterlik, H. Kataura, Y. Achiba, Eur. Phys. J. B 22 (2001) 307.

[15] A. Jorio, A.G. Souza Filho, G. Dresselhaus, M.S. Dresselhaus, A.K. Swan, M.S. Unlu, B.B. Goldberg, M.A. Pimenta, J.H. Hafner, C.M. Lieber, R. Saito, Phys. Rev. B 65 (2002) 155412.

[16] C. Thomsen, C. Reich, Phys. Rev. Lett. 85 (2000) 5214.

[17] H. Kataura, Y. Kumazawa, Y. Maniwa, I. Umezu, S. Suzuki, Y. Ohtsuka, Y. Achiba, Synthetic Met. 103 (1999) 2555.

[18] S.D.M. Brown, A. Jorio, P. Corio, M.S. Dresselhaus, G. Dresselhaus, R. Saito, K. Kneipp, Phys. Rev. B 63 (2001) 155414.

[19] S.N. Bokova, E.D. Obraztsova, A.V. Osanchy, H. Kuzmany, U. Dettlaff-Weglikowska, S. Roth, in: S. Guceri, Y. Gogotsi, V.L. Kuznetsov (Eds.), Nanoengineered Nanofibrous Materials, Kluwer, 2004, p. 131.

[20] L.J. Ci, Z.P. Zhou, L. Song, X.Q. Yan, D.F. Liu, H.J. Yuan, Y. Gao, J.X. Wang, L.F. Liu, W.Y. Zhou, G. Wang, S.S. Xie, Appl. Phys. Lett. 82 (2003) 3098.

[21] H. Ohtsuka, T. Tabata, O. Okada, L.M.F. Sabatino, G. Bellussi, Catal. Lett. 44 (1997) 265.

[22] R. Martel, H.R. Shea, P. Avouris, J. Phys. Chem. B 103 (1999) 7551.

[23] R. Martel, H.R. Shea, P. Avouris, Nature 398 (1999) 299.